A reconstruction of warm water inflow to Upernavik Isstrøm since AD 1925 and its relation to glacier retreat

Flor Vermassen[1,2], Nanna Andreasen[1,3], David J. Wangner[1,2], Nicolas Thibault[3], Marit-Solveig Seidenkrantz[4], Rebecca Jackson[1], Sabine M. Schmidt[5], Kurt H. Kjær[2], Camilla S. Andresen[1].

5   [1]Department of Glaciology and Climate, Geological Survey of Denmark and Greenland (GEUS), Copenhagen, Denmark;

[2]Centre for GeoGenetics, Natural History Museum, University of Copenhagen, Copenhagen, Denmark;

[3]Department of Geosciences and Natural Resource Management, University of Copenhagen, Copenhagen, Denmark;

[4]Institute for Geoscience, Aarhus University, Aarhus, Denmark

10   [5]CNRS, OASU, EPOC, UMR5805, Pessac Cedex, France

Correspondence to: Flor Vermassen (flv@geus.dk)

Abstract. The mass loss from the Greenland Ice Sheet has increased over the past two decades. Marine-terminating glaciers contribute significantly to this mass loss due to increased melting and ice discharge. Rapid retreat periods of these tidewater glaciers have been linked to the concurrent inflow of warm, Atlantic derived waters. However, little is known about the
15   variability of Atlantic-derived waters within these fjords, due to a lack of multi-annual, in situ measurements. Thus, to better understand the potential role of ocean warming on glacier retreat, reconstructions that characterize the variability of Atlantic water inflow to these fjords are required. Here, we investigate foraminiferal assemblages in a sediment core from Upernavik Fjord, West Greenland, in which the major ice stream Upernavik Isstrøm terminates. We investigate the environmental characteristics that control species diversity and derive that it is predominantly controlled by changes in bottom water
20   variability. Hence, we provide a reconstruction of Atlantic water inflow to Upernavik Fjord, spanning the period 1925-2012. This reconstruction reveals peak Atlantic water inflow during the 1930s and again after 2000, a pattern that is similar to the Atlantic Multidecadal Oscillation (AMO). We compare these results to historical observations of front positions of Upernavik Isstrøm. This reveals that inflow of warm, Atlantic-derived waters indeed likely contributed to high retreat rates in the 1930s and after 2000. However, moderate retreat rates of Upernavik Isstrøm also prevailed in the 1960s/1970s, showing that retreat
25   continued despite reduced Atlantic water inflow, albeit at a lower rate. Considering the link between bottom water variability and the AMO in Upernavik Fjord and the fact that a persistent negative phase of the AMO is expected for the next decade, Atlantic water inflow into the fjord may decrease in the next ~10 years.

1 Introduction

Mass loss from the Greenland Ice Sheet (GrIS) has accelerated over the past two decades, raising its contribution to the ongoing global sea-level rise. Currently about one third of the mass loss is attributed to dynamic loss in the form of ice discharge from large tidewater glaciers (van den Broeke et al., 2016). The processes controlling the instability of these glaciers are however

5 still not well understood, and therefore the capability of computational models to predict the rate of future mass loss remains limited. During the early 2000's a rapid retreat of tidewater glaciers along the south-eastern (SE) sector of the GrIS was observed, followed by retreat of glaciers in the north-western (NW) sector (Joughin et al., 2013; Khan et al., 2010; Kjær et al., 2012; Straneo et al., 2013). This retreat coincided with a warming of the ocean waters in SE and NW Greenland and has led to the hypothesis that shifting ocean currents exert a major control on the dynamic behaviour of these glaciers (Holland et al.,

10 2008; Straneo et al., 2013). Several studies have examined past ice-ocean interactions to investigate the importance of ocean forcing on a longer timescale (Andresen et al., 2010, 2011, 2017; Dyke et al., 2017; Lloyd et al., 2011; Wangner et al., 2018) but few have the temporal resolution needed for an in-depth study of (sub-)decadal dynamics (Drinkwater et al., 2014). In West-Greenland specifically, only a few observations or detailed reconstructions of bottom water temperatures throughout the 20th century exist (Lloyd et al., 2011; Ribergaard et al., 2008). Sediment records in Greenlandic fjords with marine-terminating

15 glaciers are usually characterised by relatively high sedimentation rates (Dowdeswell et al., 1998), thus allowing environmental reconstructions with a high temporal resolution. Benthic foraminiferal communities, in particular, are sensitive to environmental conditions and shifts in species assemblages can be used to reconstruct relative changes of bottom water masses (Murray, 2006).

Here we investigate foraminiferal assemblages in a sediment core in Upernavik Fjord, NW Greenland. We evaluate which

20 environmental factors influence species assemblages and reconstruct Atlantic water inflow to Upernavik Isstrøm since 1925. These results are compared to historical records of the Upernavik Isstrøm ice front retreat in order to assess whether periods of increased Atlantic water inflow in the fjord are associated with glacier retreat.

2 Study area and previous research

25 Upernavik Fjord has a length of ~60 km and is 5-7 km wide. The fjord floor has been mapped with a Multibeam Echo Sounder System (MBES) as part of NASA's Oceans Melting Greenland mission (NASA OMG Mission, 2016). The outer part of the fjord is characterised by steep side walls and a flat fjord floor at ~900m water depth.

Recent CTD measurements have revealed a stratified water column in Upernavik Isfjord, with evidence for warm water entrainment at depth near the glacier front (below ~250m) (Andresen et al., 2014; Fenty et al., 2016). This warm water layer

30 flows below a colder and fresher surface water layer. The stratification is the result of two ocean currents that influence the hydrography of the fjord (Fig. 1). The West Greenland Current flows northward as a subsurface current along the West-Greenland margin and transports relatively warm, saline waters that originate from the Irminger Current in the Atlantic Ocean

(mean temperature >4°C, mean salinity >34.91 psu; Myers et al., 2007. Due to the relatively shallow waters of the shelf, the WGC also forms the bottom waters in this region. Along its path, this water mass mixes with colder and fresher waters of the East Greenland Current, which transports cold and less saline waters from the Arctic Ocean as a near-surface current (<1°C, <34.9 psu; Sutherland and Pickart, 2008)). Local waters, heavily influenced by meltwater from the Greenland Ice Sheet, are

5   found at the very surface. The West Greenland Current reaches Upernavik Fjord via a deep trough (~700m) (Fig. 1).

Upernavik Isstrøm is a major ice stream in NW Greenland, draining a significant part of the Greenland Ice sheet (~65,000 km2) (Haubner et al., 2018) (Fig. 1). In 1886, Upernavik Isstrøm was characterised by a single glacier front, but since then it has retreated into different branches of the fjord (Weidick et al. 1958). Currently, four glaciers calve into the fjord waters (named Upernavik 1 to 4, see Fig. 2).

10   The Upernavik Isstrøm is one of few outlet glaciers in Greenland with historical observations of its ice-front position throughout the 20th century. A compilation of these shows retreat of Upernavik Isstrøm starting in 1930 (Khan et al., 2013; Weidick, 1958). These observations were used to prescribe a 3D model that estimated mass loss between 1849-2012 (Haubner et al., 2018). This revealed a period with near zero mass loss between 1849–1932, mass loss dominated by ice dynamical flow between 1932-1998, and mass loss that was twice that of any earlier period between 1998-2012. A study of aerial photographs

15   revealed a shift in mass loss dominated by thinning of the southern glaciers between 1985-2005, to mass loss mainly due to thinning of the northern glaciers between 2005-2010 (Kjær et al., 2012). Asynchronous behaviour of the different glaciers after 2005 was also described by Larsen et al. (2016); this study showed an acceleration of Upernavik 1 and Upernavik 2 in 2006 and 2009, respectively, while the southern glaciers Upernavik 3 and 4 remained stable. The spatial variability of IRD in Upernavik fjord and its relation to glacier retreat was investigated by Vermassen et al. (under review).

3 Methods

3.1. Core collection

Sediment core POR13-05 (172 cm, 72.945 N, 55.620 W) was collected from 900 m water depth in August 2013 during a cruise with *R/V Porsild*. Coring was undertaken with a Rumohr corer (Meischner and Ruhmohr, 1974). This type of device is

25   specifically designed to avoid sediment disturbance during coring, thereby ensuring preservation of the core top. Foraminifera assemblages were investigated in the top 50 cm of the core. The grain-size analysis and age model of this core were previously presented in Vermassen et al. (under review).

3.2. Grain-size analysis

The core was sampled continuously every centimetre for grain size analysis. In order to calculate the water content, sample

30   weight was measured before and after freeze-drying. Wet-sieving was performed on all samples, separating them into three grain-size fractions (<63 µm, 63-125 µm, and >125 µm). For the >125 µm fraction, singular pebbles >0.01g were discarded

from the measurements to avoid distortion of the analysis due to the occurrence of an individual large grain (Wangner et al., 2018). The different fractions were weighed and the individual percentages were calculated relative to the total dry weight.

3.3. Age model

Sediment ages were determined with ^{210}Pb dating. Seven samples each obtained from a 1 cm interval were freeze-dried and 4–6 g of dry sediment was then conditioned in sealed vials. A well-type gamma detector Cryocycle-I (Canberra) at the laboratory UMR5805 EPOC (University of Bordeaux, France) was used to measure ^{210}Pb, ^{226}Ra and ^{137}Cs. Estimated errors of radionuclide activities are based on 1 standard deviation counting statistics. Excess ^{210}Pb (^{210}Pb$_{xs}$) is calculated by subtracting the activity supported by its parent isotope, ^{226}Ra, from the total ^{210}Pb activity in the sediment. The CF-CS (constant flux, constant sedimentation) model was applied to calculate a sedimentation rate. The sedimentation rate was then used to calculate sediment ages. The sediment surface was assumed to represent the year of core acquisition (2013).

3.4. Foraminifera analysis

Sediment slices were sub-sampled so that they contained an estimated amount of ~300-~500 tests. Foraminiferal assemblage analysis was performed on 26 samples from the top 50 cm of the core. This corresponds to a time-resolution of ~4 years between samples. Samples were soaked overnight in a light alkaline solution (Na$_2$CO$_3$, 15g/l) to disintegrate silt and clay clumps in the samples. Subsequently, they were wet-sieved with a 63 μm sieve and stored with a storage solution, consisting of distilled water, ethanol and sodium carbonate. In order to preserve the most fragile species, the foraminifera were wet-counted (Bergsten, 1994). This also allowed the identification of organic linings, mainly belonging to *E. clavatum*. A minimum of 300 tests was counted for each sample. Based on previous research, species were categorised into three groups: warm water indicators, cold water indicators, and those with no specific environmental preference (see Table S1). A principal component analysis (PCA) of species abundances >0.5% was performed with the software PAST (Hammer et al., 2001). This was done to simplify analysis and visualisation of the variation within the dataset. Abundances were normalised before the PCA analysis by calculating z-scores to avoid skewing of the data by species with large abundances. Correlations of time series were calculated in Microsoft Excel using the Pearson correlation function.

4 Results

4.1. Core lithology and sedimentology

Visual observations of the core section reveal a brown mud (code 10 R 5/6 (Munsell, 1912)) with sub-angular to sub-rounded pebbles interspersed throughout the core (Fig. 3). The split core surface shows no sign of bioturbation, confirmed by the X-

ray image and the age model. Grain-size measurements and the X-ray image show that the lower part (172-90 cm) of core POR13-05 is characterised by an alternation of mud-supported diamicton versus homogeneous mud without pebbles. The mid-section of the core contains a thick, sandy turbidite, characterized by a fining-upwards trend (90–70 cm), capped by a muddy, pebble-free unit at 68-53 cm (Fig. 3). The upper-part of the core (53–0 cm) is composed of massive, mud-supported diamicton, predominantly comprising of clay (>90 %) interspersed with larger clasts up to pebble size.

4.2. Age model

The 50 cm display a logarithmic decay of ^{210}Pb, indicating continuous sedimentation (Fig. 4). Based on the CF-CS model a sedimentation rate of 0.58 cm/yr was derived. This corresponds to an age of 1925 ± yr at 50 cm depth. The turbidite at 70-50 cm hinders dating further downcore.

4.3. Foraminifera assemblage variability

A total of 35 benthic foraminiferal species were identified, of which 16 species are calcareous and 19 agglutinated. Three planktonic species were identified in four samples, but these are excluded from the calculations. We base our habitat categorisation on studies from Disko Bay (Lloyd et al., 2007, 2011, Perner et al., 2011, 2013; Wangner et al., 2018), the central West-Greenland slope (Jennings et al., 2017) and continental shelf (Sheldon et al., 2016). The percentage-distribution of each species is calculated relative to the total benthic assemblage, i.e. both calcareous and agglutinated specimens (Fig. 5). Species representing >0.5% of the total assemblage are presented in Fig. 5. The counts and percentages of species with lower abundances can be found in the supplementary material. The agglutinated assemblage >0.5% comprises 1 species that is indicative of Atlantic waters (*Adercotryma glomerata*), the others are indicative of Arctic waters or are non-indicative (Table S1). Within the calcareous assemblage (>0.5%), 2 species are indicative of warm water conditions, 3 of cold water conditions, and 2 are non-indicative (Table S2). Agglutinated species generally dominate the assemblage and range between 45-99%. Among these *Textularia earlandi* and *Spiroplectammina biformis* are the most abundant species, with a median of 17% and 14% respectively. The other agglutinated species are markedly less abundant with medians lower than 5%. The most abundant calcareous species are *Stainforthia feylingi* and *Elphidium clavatum*, with a median of 16% and 4% of the total count, respectively. The median percentage of other calcareous species is lower than 2%.

The variability in species assemblage is broadly characterised by three intervals. Between 50 and 25 cm, the percentage of calcareous species is high, varying between 40-70% (Fig. 5). Between 25 and 12 cm, calcareous abundances are low (<20%), with almost none present between 16-12 cm. Between 12 and 0 cm, the amount of calcareous species increases again up to 40%, and high values of 40-50% occur between 6 and 0 cm. The concentration of foraminifera, expressed as counts/gram of wet sediment, varies generally between 60-150 counts/g. Outliers with anomalous low and high counts/g are present at 45 cm (21 counts/g) and 1 cm (308 counts/g), respectively. The amount of organic linings per gram shows a trend that is inversely proportional to the percentage of calcareous species.

4.4. PCA analysis

Principal components 1 and 2 explain 28.6% and 16.8% of the variance in the dataset, respectively. The loadings plot reveals a clustering of broadly three groups of foraminiferal species (Fig. 6). The first group consists of calcareous species characterised by strongly negative PC1 loadings (group 1). This group consists of both cold and warm water indicators. The second group consists of cold-water agglutinated species, characterised by strongly positive PC1 loadings (group 2). The third group consists mostly of species that are not indicative of a specific water mass (group 3). These species have low loadings for PC1 and strongly negative loadings for PC2.

5 Discussion

5.1. Environmental controls on species abundance in Upernavik Fjord

Foraminifera species are sensitive to changes in water depth, substrate, bottom water characteristics (temperature, salinity) and nutrient flux (Lloyd, 2006; Murray, 2006). Species displaying the same pattern of variability respond to similar environmental changes. To determine which environmental parameters control species abundances in Upernavik Fjord we compare our PCA results with the ecological preferences of species as suggested in the literature.

PC 1 is dominated by the opposition in the trends observed in the abundance of agglutinated and calcareous species (Fig. 6). The fact that the agglutinated species *T. torquata, S. biformis, P. bipolaris, and R. turbinatus* show similar trends is expected since the literature suggests they thrive in similar environmental conditions, i.e. cold, arctic waters (Table S1). However, it should be noted that while the investigations that we compiled attribute these species to Arctic waters, some of these species have also been identified in sediments in Gullmar Fjord, SE Sweden (Höglund, 1947; Polovodova Asteman et al., 2013). Therefore, we add a cautionary note that these species could in fact be more cosmopolitan than commonly assumed. Nevertheless, to remain consistent with recent studies in West Greenland we consider them here indicative of Arctic waters

In the calcareous assemblage the Arctic-water indicators *S. concava* and *S. feylingi* display similar trends as the (chilled) Atlantic water indicators *N. labradorica* and *N. auricula.* We propose that their similar trends can be explained because these species have been suggested as indicators of high-productivity environments (except *N. auricula*), i.e. they thrive when the flux of organic material from surface waters is high (Jennings et al., 2017 and references therein). This is also evidenced because of the similarity with the pattern of abundance of *B. pseudopunctata*; a species that is considered indifferent to changes in Atlantic/Arctic waters but sensitive to surface water productivity (Sheldon et al., 2016). Thus, the PCA results suggest that the assemblage diversity is influenced both by environmental factors that control the ratio of agglutinated/calcareous species, as well as by changes of the primary productivity in the fjord.

The opposition between calcareous and agglutinated foraminifera is not surprising as both groups have different environmental preferences and preservation potential; similar patterns in shifts between agglutinated and calcareous species are commonly seen in Arctic records (Andresen et al., 2012; Seidenkrantz et al., 2007). An important factor controlling the abundance of

calcareous foraminifera is the concentration of HCO_3^{2-} in the ambient water. In cold waters the calcification process may be limited by a lack of HCO_3^{2-}, while warmer waters promote calcification. In addition and perhaps more importantly, the preservation of calcareous specimens can be influenced by post-mortem dissolution. Colder waters contain more CO_2 and are thus less alkaline than warmer waters; this promotes dissolution of calcareous tests. Test dissolution is common in Arctic

5   waters and is likewise important in Upernavik Fjord. The fact that post-mortem dissolution plays an important role in explaining the patterns of our dataset is further supported by the inverse relationship between the percentage of calcareous species and foraminiferal test linings (Fig. 6). Organic linings are less susceptible to dissolution than calcareous tests and remain better preserved under corrosive conditions. Hence, during periods with relatively warm waters entering the fjord, carbonate test are better preserved, whereas colder water conditions will result in a higher abundance of organic linings. Warm

10   subsurface (bottom) waters prevail in the fjord when the Atlantic-derived portion of the West Greenland Current is high. Conversely, when the Atlantic portion of the West Greenland Current is low and contribution of Arctic-derived waters (i.e. East Greenland Current) is high, colder bottom waters will corrode calcareous benthic foraminifer tests. Therefore, we suggest that the abundance of calcareous foraminifera represents here a proxy for the inflow of warm, Atlantic-derived waters to the fjord. This interpretation is strengthened by a similar study in the Ameralik Fjord (SW Greenland) where the percentage of

15   calcareous foraminifera was used as a proxy for the influx of warm, Atlantic-derived waters (Seidenkrantz et al., 2007). In that study it was suggested that calcification of benthic foraminifera tests is prevented at times of sea-ice growth due to the associated formation of CO_2 rich brine waters. In Upernavik Fjord we also suggest an influence of bottom water alkalinity on foraminifer assemblage, but it should be noted that the mechanism by which corrosive cold water currents circulate in the fjord is probably different. In contrast to Ameralik Fjord, the absence of a sill separating Upernavik Fjord from the Baffin Bay

20   allows a more direct connection to the open ocean. This permits shelf currents to enter the fjord, and together with outflowing surface meltwater this results in a strong circulation in the fjord (buoyancy-driven circulation; Cowton et al., 2016). Thus, bottom waters are likely well-ventilated and influenced directly by inflowing bottom waters rather than by the sinking of brine waters.

Furthermore, we infer an influence of Atlantic waters on the nutrient level in the fjord, and hence on the composition of benthic

25   calcareous species assemblage. Recent research showed that primary productivity in a fjord with a marine-terminating glacier is predominantly controlled by rising subsurface meltwater plumes entraining ambient nutrient-rich deep water to the surface (Meire et al., 2017). Productivity in a fjord with a land-terminating glacier (Young Sound, NE Greenland) and one with marine-terminating glaciers (Godthåbsfjord, SW Greenland) were compared, revealing that the limiting amount of nutrients available for phytoplankton in these fjords is predominantly delivered through upwelling of Atlantic-derived waters (Meire et

30   al., 2017). Periods with more Atlantic water inflow would thus lead to a higher primary productivity, which in turn would favour meso- and eutrophic benthic species at the sea-floor. Such a mechanism would thus explain the similar abundance trends of the Atlantic indicators *N. labradorica and N. auricula* together with the cold-water indicators *S. feylingi* and *S. concava* and with the mesotrophic indicator *B. Pseudopuncata*, all species essentially responding here to variations in bottom-water nutriency (Fig. 5 and 6).

In summary, we suggest that the dominant control on the composition of the foraminiferal assemblage essentially relates to (post-mortem) dissolution of calcareous species, controlled by variations in the alkalinity of the West Greenland Current and associated contribution of Atlantic water. As a second control, an increased inflow of Atlantic waters results in more upwelling of nutrients and thus in higher primary productivity, favouring benthic species that thrive under a high supply of organic matter

5   from surface waters. Based on these results, we use the percentage of calcareous foraminifera as a proxy for Atlantic water inflow to Upernavik Fjord.

5.2. Comparison to climatic records

The foraminiferal record suggests warm bottom water masses during 1920-1960, interrupted by a minor cooling around 1940 (Fig. 7). After 1960 a stronger cooling occurs with minimal temperatures between 1980 and the early '90s. From the mid '90s

10   onwards a rapid warming occurs, reaching peak values after 2005. Our reconstructed record is supported by the measured bottom water temperatures at Fylla Banke (400-600m), located offshore Nuuk in SW Greenland, which show a similar pattern (Fig. 1 and 7; Ribergaard et al., 2008). This gives confidence in our reconstruction and confirms that bottom water changes in Upernavik Fjord are linked to the variability of the West-Greenland Current.

A previous foraminifera-based reconstruction of Atlantic-water influx in Disko Bugt (Lloyd et al., 2011) also shows an overall

15   comparable pattern, except for the period 1950-1975, during which our reconstruction of warm bottom water masses in Upernavik Fjord contrast with the colder conditions in Disko Bugt (Fig. 7). Potentially, this is related due to age uncertainties in both records, or subtle differences in the sensitivity of the foraminifer assemblages to the prevailing bottom water mass.

The pattern of bottom water variations reconstructed here is also similar to the pattern of the Atlantic Multidecadal Oscillation (NOAA ESRL, 2018; Enfield et al., 2001), with correlation coefficient r=0.42 and significance level p=0.05. The AMO is a

20   55-70 year cyclical pattern in Atlantic water temperature, usually considered as an expression of the variability of the overall Atlantic Ocean circulation (Kerr, 2000; Knudsen et al., 2011; Schlesinger and Ramankutty, 1994; Trenberth and Shea, 2006). A link between the physical oceanography of West Greenland and Atlantic SSTs has indeed been suggested previously: a positive phase of the AMO is related to an increase of warm Atlantic waters flowing towards and along the SE and W Greenland shelf (Drinkwater et al., 2014; Lloyd et al., 2011). Our data indeed supports that the AMO influences bottom water temperature

25   variability along the West Greenland shelf and shows that this influence is strong within Upernavik Fjord.

5.3. Retreat of Upernavik Isstrøm and ocean forcing

The retreat history of Upernavik Isstrøm is relatively well constrained from historical observations (Fig. 2). Nevertheless, care should be taken in interpreting this record because of the relatively low resolution for the older parts of the record. By

30   comparing this record to our reconstruction of bottom water variability we evaluate whether ocean warming was concurrent with periods of retreat throughout the 20th/21st century.

Despite differences in the timing and magnitude of the retreat of the different glaciers, they broadly share the same retreat history. High retreat rates occurred between the mid '30s and mid '40s (400-800m/yr), moderate retreat rates between 1965-1985 (~200 m/yr, except for Upernavik 3) and high retreat rates again after 2000 (>200 m/yr) (Fig. 8). The largest difference between individual glaciers occurred after 2005 when the northern glaciers Upernavik 1 and Upernavik 2 retreated and thinned

5 fast, but the southern glaciers Upernavik 3 and Upernavik 4 remained relatively stable (Kjær et al., 2012; Larsen et al., 2016) (Fig. 8).

Our reconstruction reveals that relatively warm, Atlantic-derived bottom waters prevailed in Upernavik Fjord in the 1930s and after 1995 AD. Warm water inflow may thus have triggered the substantial retreat that was observed during these periods. However, the cause of these periods of retreat cannot be attributed solely to ocean forcing since air temperatures mostly co-

10 vary with the reconstructed bottom water variability (Fig. 8). Therefore, disentangling the relative importance between oceanic and atmospheric forcing remains challenging (Straneo and Heimbach, 2013). Both processes are inherently linked not only due to a common regional forcing of both (AMO), but also because increased glacier run-off (due to warmer air temperatures) can strengthen fjord circulation and thus increase inflow of Atlantic waters (Carroll et al., 2016; Christoffersen et al., 2011). Moderate retreat rates during 1960-1985 coincided with cooling of bottom waters, showing that retreat occurred despite a

15 stabilising effect from decreasing ocean water temperatures. Instead, retreat during this period was potentially perpetuated by a negative surface mass balance (Haubner et al 2018) or potentially due to a dynamic response to variations in bed topography. Thus, these findings emphasise that the timing and magnitude of the retreat of Upernavik Isstrøm throughout the 20th/21st century is not simply a function of bottom water temperature variability but reflects a complex response to multiple forcing mechanisms.

20 Finally, we note that even when the inflow of Atlantic water to the fjord is high, variations in fjord bathymetry can determine whether the warm waters are able to perturb the glacier front(s). This could for example explain the differential response of the northern glaciers (Upernavik 1 and 2) versus the southern glaciers (Upernavik 3 and 4) after 2000 AD, as was suggested by Andresen et al. (2014). The northern glaciers (Upernavik 1 and 2) are positioned on a deep bed (~900m), whereas the southern glaciers (Upernavik 3 and 4) are positioned on a shallower bed (<400 m water depth). Because the Atlantic water

25 layer flows at 400-900m depth the southern glaciers would thus not have been affected by warming of the Atlantic layer, in contrast to the northern glaciers.

6 Conclusions

In this study, we show that the abundance and diversity of foraminifer species in the outer region of Upernavik Fjord is

30 predominantly controlled by the preservation potential of calcareous species, depending on the alkalinity of the prevailing bottom water mass, which is in turn related to variations in water temperature. Therefore, we use the percentage of calcareous species as a proxy for the inflow of the warm, Atlantic component of the West Greenland Current. This reconstruction spans

the period 1925-2012 and broadly displays the same pattern of variability as the Atlantic Multidecadal Oscillation. Comparison of our bottom water record with historical observations of glacier front positions reveals that warm subsurface waters were associated with marked retreat periods of Upernavik Isstrøm during the 1930s and after 1995 AD. Conversely, retreat of Upernavik Isstrøm during 1960-1985 was associated with cooling bottom waters, showing that this retreat was not simply a function of bottom water variability. Thus, our study shows that while warming of ocean waters in Upernavik fjord likely contributed to the retreat phases during the 1930s and early 2000s, ocean warming is not a prerequisite for retreat of Upernavik Isstrøm. The similar pattern of our bottom water reconstruction with the Atlantic Multidecadal Oscillation shows that ocean currents interacting with Upernavik Isstrøm depend on ocean circulation changes originating in the North-Atlantic, a finding that is consistent with a study in Disko Bay, located ~450km further south of our study site (Lloyd et al., 2011). This is important since it implies that the future potential oceanic forcing of Upernavik Isstrøm will depend on changes related to circulation in the North Atlantic (i.e. the AMO). Since the meridional overturning circulation strength and associated heat transport is currently declining, (Frajka-Williams et al., 2017), this may lead to cooling bottom waters during the next decade in Upernavik Fjord and most likely also other fjords in West-Greenland.

7 Acknowledgements:

This study is a contribution to the VILLUM FONDEN project 'Past and Future Dynamics of the Greenland Ice Sheet: what is the ocean hiding?' (10100).

MSS was supported by the Independent Research Fund Denmark (G-Ice project Grant No. 7014-00113B/FNU).

8 Data availability

All data produced for this study will be uploaded to Pangaea (https://www.pangaea.de/)

9 Conflicts of interest

Marit-Solveig Seidenkrantz is a co-editor-in-chief for Climate of the Past but was not involved in the editorial process of this article.

10 Author contributions

FV interpreted all data, performed sediment lab work and wrote the manuscript. NA counted foraminifer species and contributed to data interpretation. RJ and DJW helped with identification of the species and contributed to analysis of the data. NT contributed to data interpretation. CSA and KK designed the study. SS developed the age model. MSS revised the identification of the foraminiferal species and contributed to their interpretation. All co-authors contributed to the writing of the manuscript.

11 References

Andresen, C. S., Nørgaard-Pedersen, N., Jensen, J. B., Larsen, B. and Nørgaard-Pedersen, N.: Bathymetry, shallow seismic profiling and sediment coring in Sermilik near Helheimgletscher, South-East Greenland, Geol. Surv. Denmark Greenl. Bull., 20, 83–86 [online] Available from: http://www.geus.dk/publications/bull/nr20/nr20_p083-086.pdf, 2010.

Andresen, C. S., McCarthy, D. J., Valdemar Dylmer, C., Seidenkrantz, M.-S., Kuijpers, A. and Lloyd, J. M.: Interaction between subsurface ocean waters and calving of the Jakobshavn Isbrae during the late Holocene, The Holocene, 21(2), 211–224, doi:10.1177/0959683610378877, 2011.

Andresen, C. S., Hansen, M. J., Seidenkrantz, M.-S., Jennings, A. E., Knudsen, M. F., Norgaard-Pedersen, N., Larsen, N. K., Kuijpers, A. and Pearce, C.: Mid- to late-Holocene oceanographic variability on the Southeast Greenland shelf, The Holocene, 23(2), 167–178, doi:10.1177/0959683612460789, 2012.

Andresen, C. S., Kjeldsen, K. K., Harden, B., Nørgaard-Pedersen, N. and Kjær, K. H.: Outlet glacier dynamics and bathymetry at Upernavik Isstrøm and Upernavik Isfjord, North-West Greenland, Geol. Surv. Denmark Greenl. Bull., 31(August 2013), 79–82, 2014.

Andresen, C. S., Kokfelt, U., Sicre, M.-A., Knudsen, M. F., Dyke, L. M., Klein, V., Kaczmar, F., Miles, M. W. and Wangner, D. J.: Exceptional 20th century glaciological regime of a major SE Greenland outlet glacier, Sci. Rep., 7(1), 13626, doi:10.1038/s41598-017-13246-x, 2017.

van den Broeke, M. R., Enderlin, E. M., Howat, I. M., Kuipers Munneke, P., Noël, B. P. Y., Jan Van De Berg, W., Van Meijgaard, E. and Wouters, B.: On the recent contribution of the Greenland ice sheet to sea level change, Cryosphere, 10(5), 1933–1946, doi:10.5194/tc-10-1933-2016, 2016.

Carroll, D., Sutherland, D. A., Hudson, B., Moon, T., Catania, G. A., Shroyer, E. L., Nash, J. D., Bartholomaus, T. C., Felikson, D., Stearns, L. A., Noï¿½l, B. P. Y. and van den Broeke, M. R.: The impact of glacier geometry on meltwater plume structure and submarine melt in Greenland fjords, Geophys. Res. Lett., 43(18), 9739–9748, doi:10.1002/2016GL070170, 2016.

Christoffersen, P., Mugford, R. I., Heywood, K. J., Joughin, I., Dowdeswell, J. A., Syvitski, J. P. M., Luckman, A. and Benham, T. J.: Warming of waters in an East Greenland fjord prior to glacier retreat: Mechanisms and connection to large-scale atmospheric conditions, Cryosphere, 5(3), 701–714, doi:10.5194/tc-5-701-2011, 2011.

Dowdeswell, J. A., Elverhøi, A. and Spielhagen, R.: Glacimarine sedimentary processes and facies on the Polar North Atlantic margins, Quat. Sci. Rev., 17(1–3), 243–272, 1998.

Drinkwater, K. F., Miles, M., Medhaug, I., Otterå, O. H., Kristiansen, T., Sundby, S. and Gao, Y.: The Atlantic Multidecadal Oscillation: Its manifestations and impacts with special emphasis on the Atlantic region north of 60°N, J. Mar. Syst., 133, 117–130, doi:10.1016/j.jmarsys.2013.11.001, 2014.

Dyke, L. M., Andresen, C. S., Seidenkrantz, M.-S., Hughes, A. L. C., Hiemstra, J. F., Murray, T., Bjørk, A. A., Sutherland, D. A. and Vermassen, F.: Minimal Holocene retreat of large tidewater glaciers in Køge Bugt, southeast Greenland, Sci. Rep., 7(1), doi:10.1038/s41598-017-12018-x, 2017.

Enfield, D. B., Mestas-Nuñez, A. M. and Trimble, P. J.: The Atlantic multidecadal oscillation and its relation to rainfall and river flows in the continental U.S, Geophys. Res. Lett., doi:10.1029/2000GL012745, 2001.

Fenty, I., Willis, J., Khazendar, A., Dinardo, S., Forsberg, R., Fukumori, I., Holland, D., Jakobsson, M., Moller, D., Morison, J., Münchow, A., Rignot, E., Schodlok, M., Thompson, A., Tinto, K., Rutherford, M. and Trenholm, N.: Oceans Melting Greenland: Early Results from NASA's Ocean-Ice Mission in Greenland, Oceanography, 29(4), 72–83 [online] Available from: https://tos.org/oceanography/article/oceans-melting-greenland-early-results-from-nasas-ocean-ice-mission-in-gree, 2016.

Frajka-Williams, E., Beaulieu, C. and Duchez, A.: Emerging negative Atlantic Multidecadal Oscillation index in spite of warm subtropics, Sci. Rep., 7(1), 1–8, doi:10.1038/s41598-017-11046-x, 2017.

Haubner, K., Box, J. E., Schlegel, N. J., Larour, E. Y., Morlighem, M., Solgaard, M., Kjeldsen, K. K. and Larsen, S. H.: Simulating ice thickness and velocity evolution of Upernavik Isstrøm 1849–2012 by forcing prescribed terminus positions in ISSM, Cryosph. Discuss., (July), 1–16, doi:https://doi.org/10.5194/tc-2017-121, 2017.

Höglund, H.: Foraminifera in the Gullmar Fjord and the Skagerak, Zool. Bidr. från Uppsala, 26, 1947.

Holland, D. M., Thomas, R. H., de Young, B., Ribergaard, M. H. and Lyberth, B.: Acceleration of Jakobshavn Isbræ triggered by warm subsurface ocean waters, Nat. Geosci., 1(10), 659–664, doi:10.1038/ngeo316, 2008.

Jennings, A. E., Andrews, J. T., Ó Cofaigh, C., Onge, G. S., Sheldon, C., Belt, S. T., Cabedo-Sanz, P. and Hillaire-Marcel, C.: Ocean forcing of Ice Sheet retreat in central west Greenland from LGM to the early Holocene, Earth Planet. Sci. Lett., 472, 1–13, doi:10.1016/j.epsl.2017.05.007, 2017.

Joughin, I., Alley, R. B. and Holland, D. M.: Oceanic Forcing, , 338(6111), 1172–6, doi:10.1126/science.1226481, 2013.

Kerr, R. A.: A north atlantic climate pacemaker for the centuries., Science, 288(5473), 1984–5, doi:10.1126/science.288.5473.1984, 2000.

Khan, S. A., Wahr, J., Bevis, M., Velicogna, I. and Kendrick, E.: Spread of ice mass loss into northwest Greenland observed by GRACE and GPS, Geophys. Res. Lett., 37(6), 1–5, doi:10.1029/2010GL042460, 2010.

Khan, S. A., Kjær, K. H., Korsgaard, N. J., Wahr, J., Joughin, I. R., Timm, L. H., Bamber, J. L., Van Den Broeke, M. R., Stearns, L. a., Hamilton, G. S., Csatho, B. M., Nielsen, K., Hurkmans, R. and Babonis, G.: Recurring dynamically induced thinning during 1985 to 2010 on Upernavik Isstrøm, West Greenland, J. Geophys. Res. Earth Surf., 118(1), 111–121, doi:10.1029/2012JF002481, 2013.

5   Kjær, K. H., Khan, S. A., Korsgaard, N. J., Wahr, J., Bamber, J. L., Hurkmans, R., van den Broeke, M., Timm, L. H., Kjeldsen, K. K., Bjørk, A. A., Larsen, N. K., Jorgensen, L. T., Faerch-Jensen, A. and Willerslev, E.: Aerial Photographs Reveal Late-20th-Century Dynamic Ice Loss in Northwestern Greenland, Science (80-.)., 337(6094), 569–573, doi:10.1126/science.1220614, 2012.

Knudsen, M. F., Seidenkrantz, M. S., Jacobsen, B. H. and Kuijpers, A.: Tracking the Atlantic Multidecadal Oscillation through 10   the last 8,000 years, Nat. Commun., 2(1), 178, doi:10.1038/ncomms1186, 2011.

Larsen, S. H., Khan, S. A., Ahlstrøm, A. P., Hvidberg, C. S., Willis, M. J. and Andersen, S. B.: Increased mass loss and asynchronous behavior of marine-terminating outlet glaciers at Upernavik Isstrøm, NW Greenland, J. Geophys. Res. F Earth Surf., 121(2), 241–256, doi:10.1002/2015JF003507, 2016.

Lloyd, J. M.: Modern Distribution of Benthic Foraminifera From Disko Bugt, West Greenland, J. Foraminifer. Res., 36(4), 15   315–331, doi:10.2113/gsjfr.36.4.315, 2006.

Lloyd, J. M., Kuijpers, A., Long, A., Moros, M. and Park, L. a: Foraminiferal reconstruction of mid- to late-Holocene ocean circulation and climate variability in Disko Bugt, West Greenland, The Holocene, 17(8), 1079–1091, doi:10.1177/0959683607082548, 2007.

Lloyd, J. M., Moros, M., Perner, K., Telford, R. J., Kuijpers, A. and Mccarthy, D.: supplementary lloyd 2011 geology., 2008.

20   Lloyd, J. M., Moros, M., Perner, K., Telford, R. J., Kuijpers, A., Jansen, E. and McCarthy, D.: A 100 yr record of ocean temperature control on the stability of Jakobshavn Isbrae, West Greenland, Geology, 39(9), 867–870, doi:10.1130/G32076.1, 2011.

Meire, L., Mortensen, J., Meire, P., Juul-Pedersen, T., Sejr, M. K., Rysgaard, S., Nygaard, R., Huybrechts, P. and Meysman, F. J. R.: Marine-terminating glaciers sustain high productivity in Greenland fjords, Glob. Chang. Biol., 23(12), 5344–5357, 25   doi:10.1111/gcb.13801, 2017.

Munsell, A. . H. .: A Pigment Color System and Notation, Am. J. Psychol., 23(2), 236–244, 1912.

Murray, J. W.: Ecology and applications of benthic foraminifera., 2006.

Myers, P. G., Kulan, N. and Ribergaard, M. H.: Irminger water variability in the West Greenland Current, Geophys. Res. Lett., 34(17), 2–7, doi:10.1029/2007GL030419, 2007.

30   NOAA ESRL, Climate timeseries: AMO timeseries, https://www.esrl.noaa.gov/psd/data/timeseries/AMO/ (data accessed 03-01-2018)

Perner, K., Moros, M., Lloyd, J. M., Kuijpers, A., Telford, R. J. and Harff, J.: Centennial scale benthic foraminiferal record of late Holocene oceanographic variability in Disko Bugt, West Greenland, Quat. Sci. Rev., 30(19–20), 2815–2826, doi:10.1016/j.quascirev.2011.06.018, 2011.

Perner, K., Moros, M., Jennings, A. E., Lloyd, J. M. and Knudsen, K.: Holocene palaeoceanographic evolution off West Greenland, The Holocene, 23(3), 374–387, doi:10.1177/0959683612460785, 2013.

Polovodova Asteman, I., Nordberg, K. and Fipsson, H. L.: The Little Ice Age: Evidence from a sediment record in Gullmar Fjord, Swedish west coast, Biogeosciences, 10(3), 1275–1290, doi:10.5194/bg-10-1275-2013, 2013.

5 Ribergaard, M. H., Olsen, S. M. and Mortensen, J.: Oceanographic Investigations off West Greenland 2007., 2008.

Schlesinger, M. E. and Ramankutty, N.: An oscillation in the global climate system of period 65–70 years, Nature, 367(6465), 723–726, doi:10.1038/367723a0, 1994.

Seidenkrantz, M.-S., Aagaard-Sørensen, S., Sulsbruck, H., Kuijpers, A., Jensen, K. G. and Kunzendorf, H.: Hydrography and climate of the last 4400 years in a SW Greenland fjord: implications for Labrador Sea palaeoceanography, The Holocene,

10 17(3), 387–401, doi:10.1177/0959683607075840, 2007.

Sheldon, C., Jennings, A. E., Andrews, J. T., Ó Cofaigh, C., Hogan, K., Dowdeswell, J. A. and Seidenkrantz, M. S.: Ice stream retreat following the LGM and onset of the west Greenland current in Uummannaq Trough, west Greenland, Quat. Sci. Rev., 147, 27–46, doi:10.1016/j.quascirev.2016.01.019, 2016.

Straneo, F. and Heimbach, P.: North Atlantic warming and the retreat of Greenland's outlet glaciers., Nature, 504(7478), 36–

15 43 [online] Available from: http://www.ncbi.nlm.nih.gov/pubmed/24305146, 2013.

Straneo, F., Heimbach, P., Sergienko, O., Hamilton, G., Catania, G., Griffies, S., Hallberg, R., Jenkins, A., Joughin, I., Motyka, R., Pfeffer, W. T., Price, S. F., Rignot, E., Scambos, T., Truffer, M. and Vieli, A.: Challenges to understanding the dynamic response of Greenland's marine terminating glaciers to oceanic and atmospheric forcing, Bull. Am. Meteorol. Soc., 94(8), 1131–1144, doi:10.1175/BAMS-D-12-00100.1, 2013.

20 Sutherland, D. A. and Pickart, R. S.: The East Greenland Coastal Current: Structure, variability, and forcing, Prog. Oceanogr., 78(1), 58–77, doi:10.1016/j.pocean.2007.09.006, 2008.

Trenberth, K. E. and Shea, D. J.: Atlantic hurricanes and natural variability in 2005, Geophys. Res. Lett., doi:10.1029/2006GL026894, 2006.

Vermassen, F., Wangner, D. J., Dyke L. M., Cordua, A., Schmidt, S. Haubner, K., Kjær, K. H., and Andresen, C. S. Evaluating

25 ice-rafted debris as a proxy for iceberg calving – results from Upernavik Isfjord. *Manuscript under revisions for the Journal of Quaternary Science*

Wangner, D. J., Jennings, A. E., Vermassen, F., Dyke, L. M., Hogan, K. A., Schmidt, S., Kjær, K. H., Knudsen, M. F. and Andresen, C. S.: A 2000-year record of ocean influence on Jakobshavn Isbræ calving activity, based on marine sediment cores, Holocene, 28(11), 1731 –1744, doi:10.1177/0959683618788701, 2018.

30 Weidick, A.: Frontal Variations at Upernaviks Isstrøm in the Last 100 Years, Meddelser fra Dansk Geol. Foren. København, 14, 52–60, 1958.

11 Figures
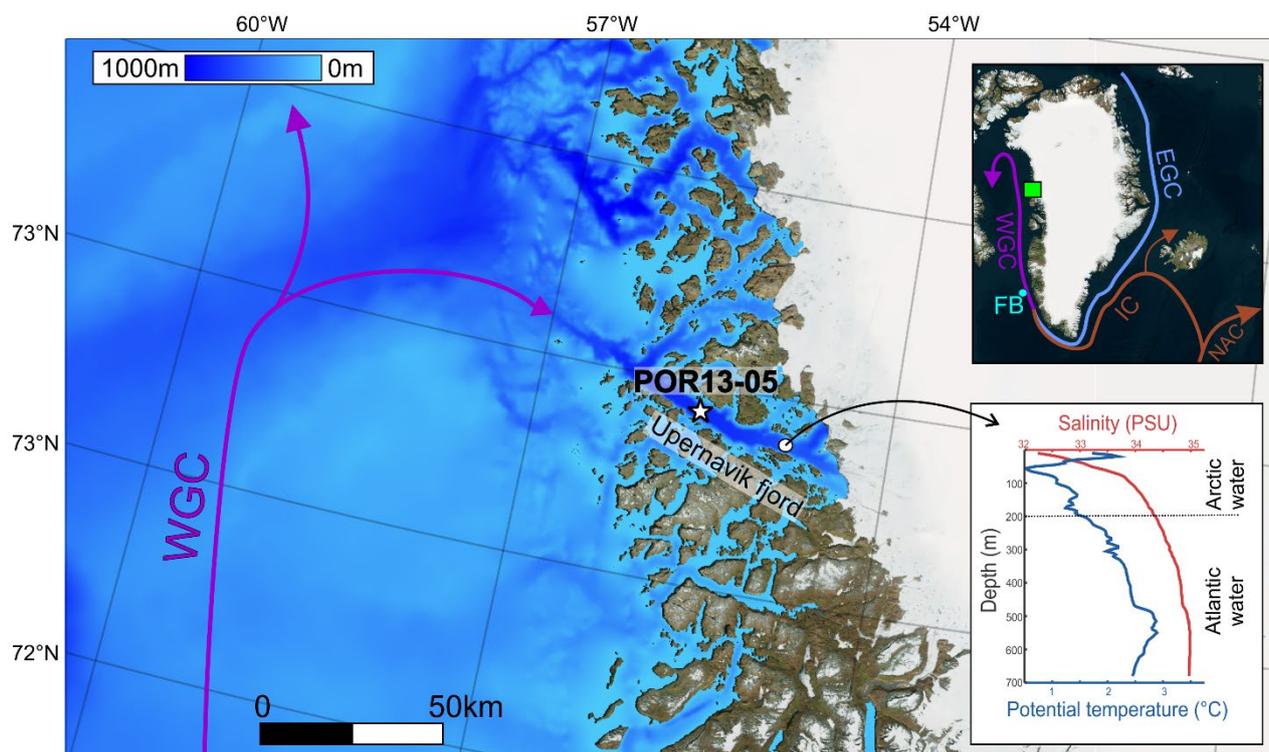
Fig 1. Position of core site POR13-05 (star) in Upernavik Fjord together with the surrounding bathymetry (Morlighem et al.,

2017). The inset figure indicates the ocean currents around Greenland (Bing satellite map, 2017). IC = Irminger Current, EGC=

5   East Greenland Current, WGC = West Greenland Current, NAC= North Atlantic Current, FB= Fylla Banke. The green box in

the inset marks the position of Upernavik Fjord, the light blue circle marks the position Fylla Banke.
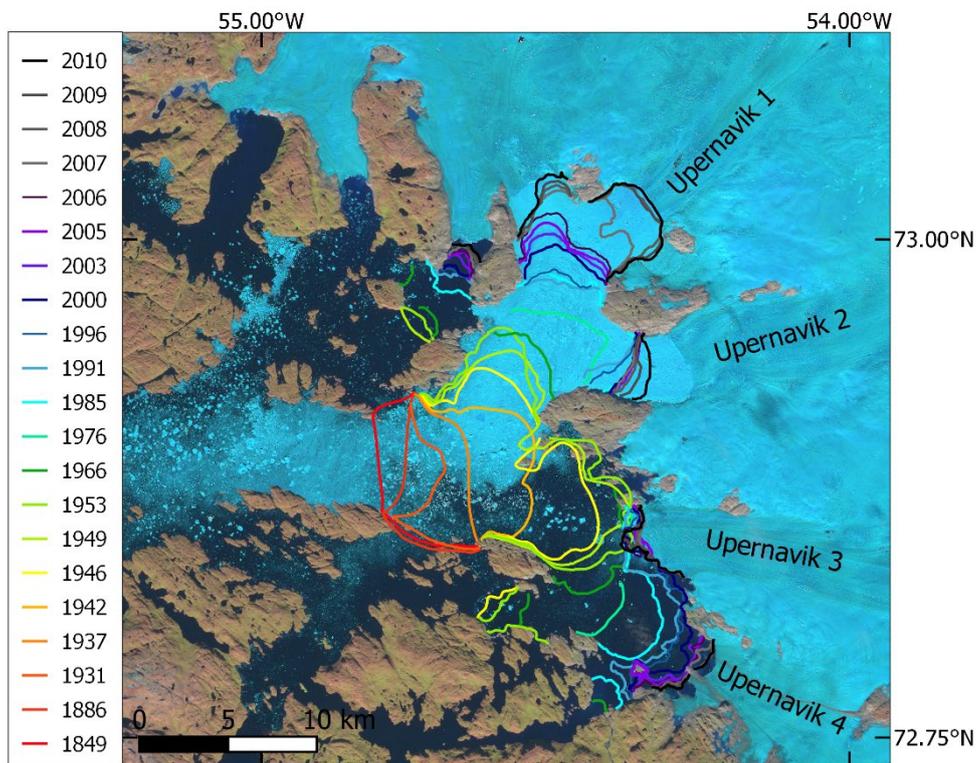
Fig.2. Satellite image (2018-07-31, Sentinel-2B) with the historical record of front observations of Upernavik Isstrøm (Weidick, 1958; Khan et al., 2013; Andresen et al., 2014).
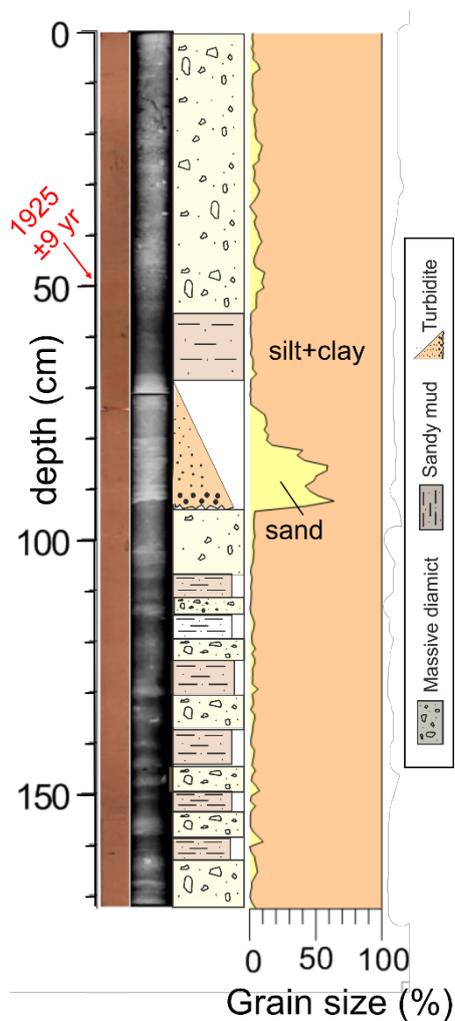
Fig 3. Linescan and X-Ray image of sediment core POR13-05, together with grain-size measurements. The top 50 cm was dated with the ^{210}Pb method.
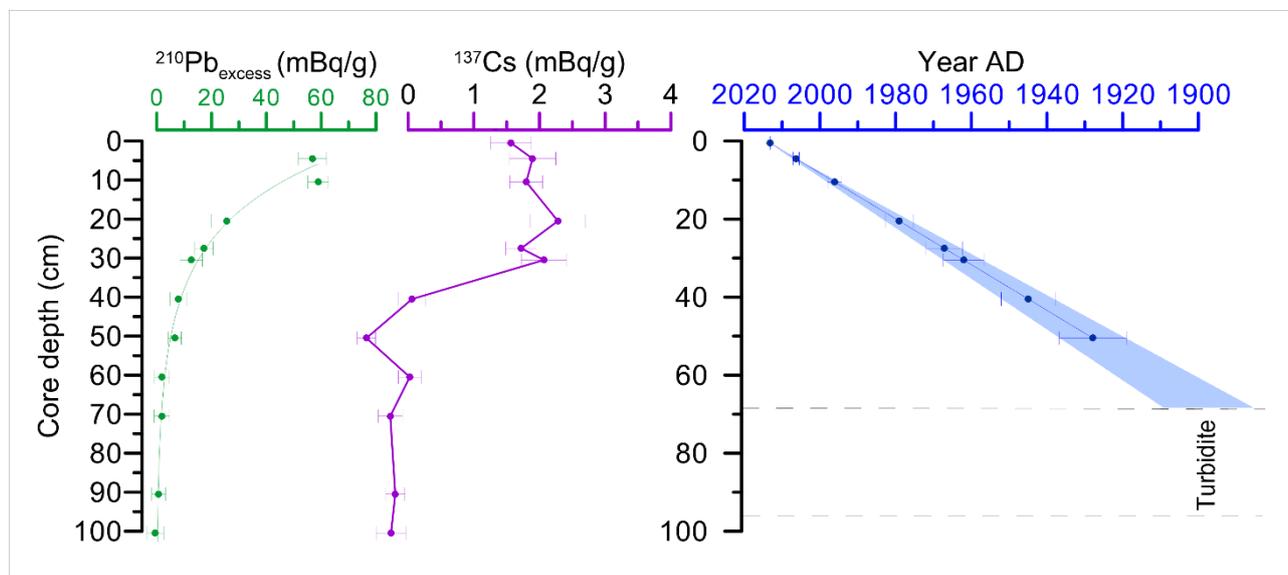
Fig. 4. Left) Measurements of $^{210}Pb_{xs}$ and ^{137}Cs according to core depth. Right) Age model calculated with the CS-CF model.
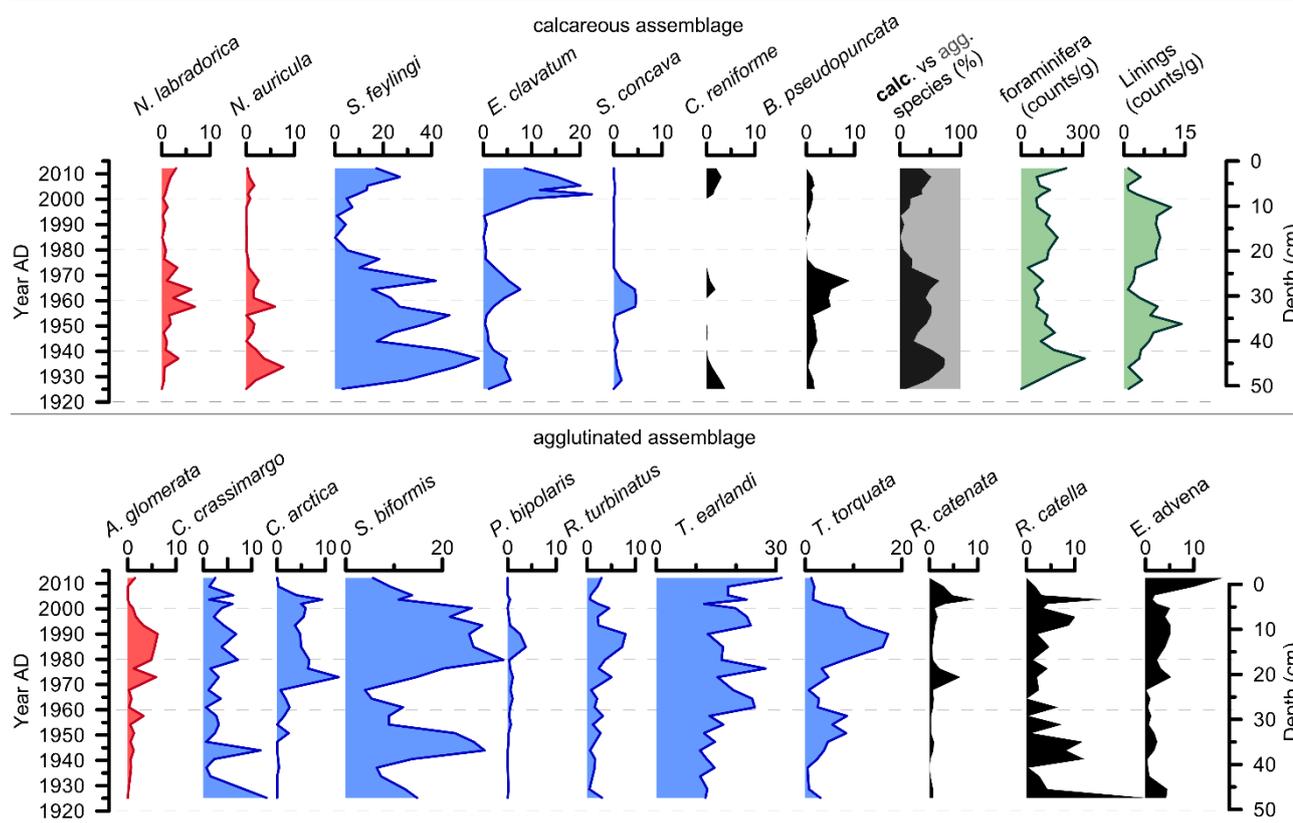
Fig. 5. Abundances of calcareous species (top) and agglutinated species (bottom), plotted versus age/depth. Abundances are calculated relative to the total counts of benthic foraminifera. Red colors indicate (chilled) Atlantic water indicator species, blue colors represent Arctic water indicators. Only species representing >0.5% of the total assemblage are shown. Total count of foraminifera and organic linings per gram are also indicated (green, top).
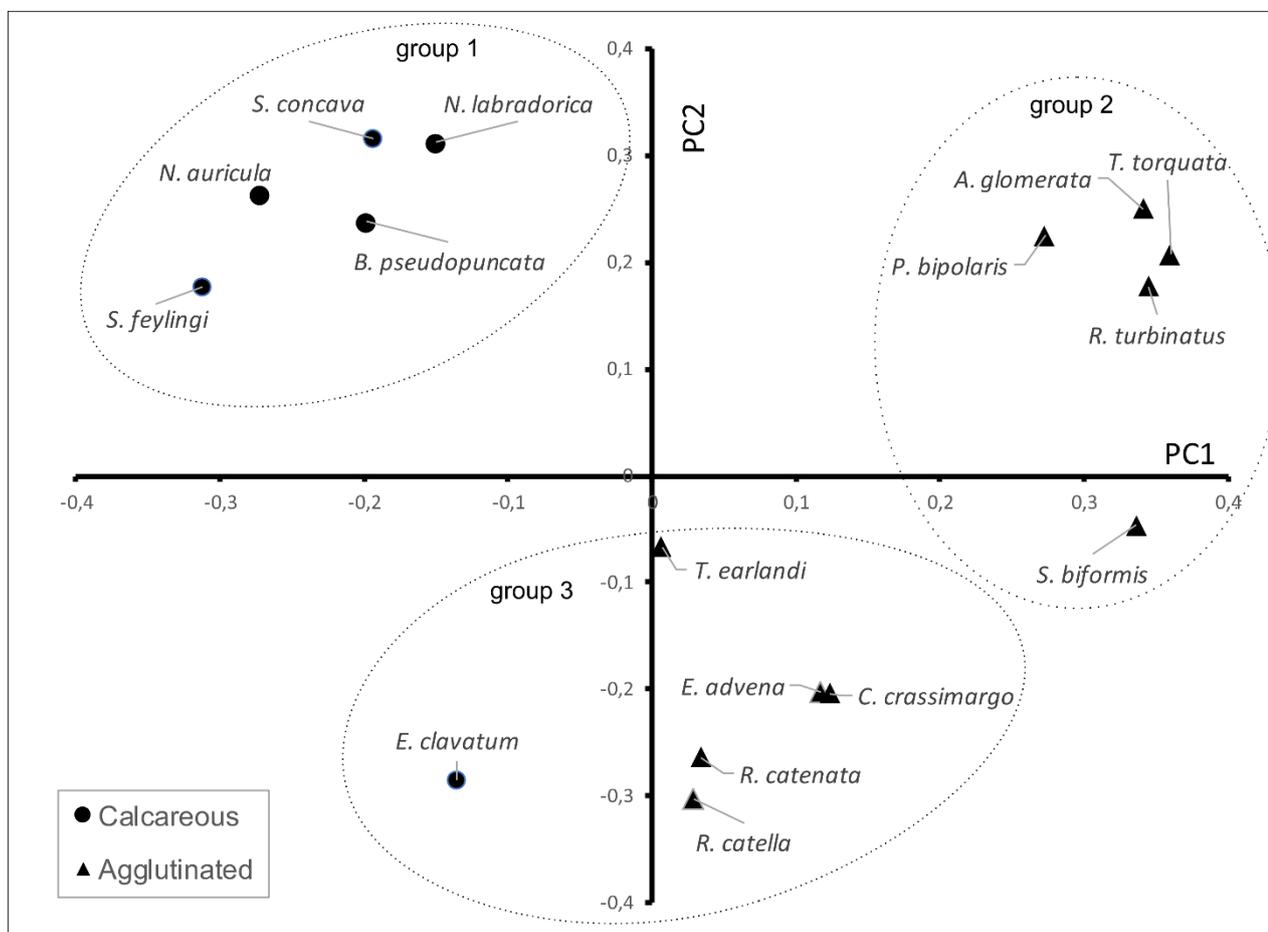
Fig. 6. Loadings plot resulting from principal component analysis. PC1 and PC2 explain 28.6% and 16.8% of the variance, respectively. Only species representing >0.5% of the total amount of counted tests were taken into account for PCA analysis.
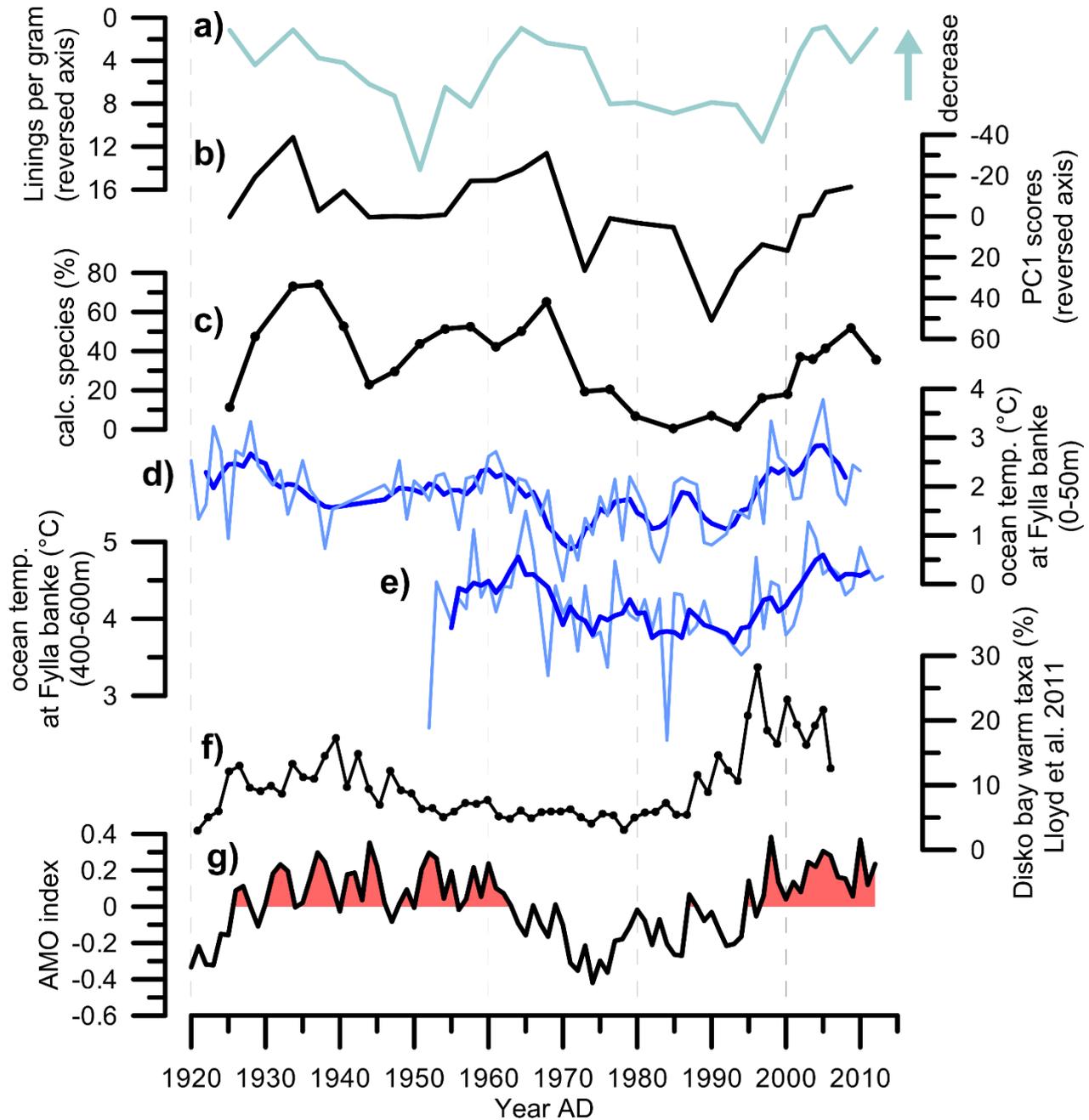
Fig. 7. Comparison of results from this study with climate records and reconstructions from West-Greenland and the Atlantic Multidecadal Oscillation (AMO). a) Number of organic linings per gram b) Scores of PC1 based on analysis of species abundances. C) Percentage of calcareous foraminifera. d) Water temperatures (0-40m, June) measured from trawl surveys at Fylla Banke, data before 1950 were extended back to 1861 based observations from a wider area (Ribergaard et al., 2008).

Dark blue line indicates the 3-year running average e) Measured temperatures at Fylla Banke (400-600m). Dark blue line indicates the 3-year running average f) Percentage of Atlantic water indicators from a benthic foraminifera study in Disko Bay, West Greenland (Lloyd et al., 2011). g) AMO index is based on the definition by Enfield et al. (2001).
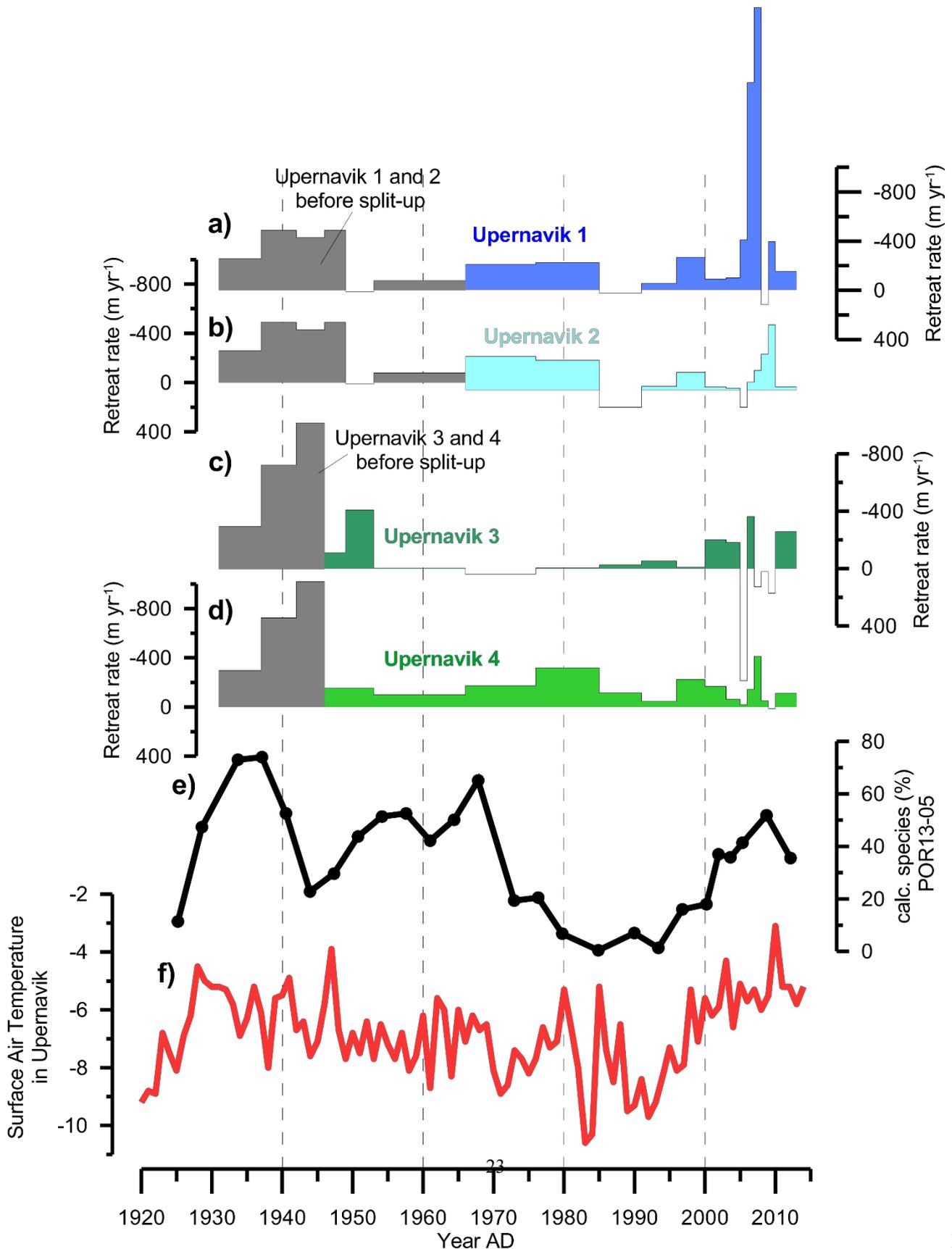
Fig.

8. Comparison of retreat rates of Upernavik Isstrøm's glaciers (Andresen et al., 2014) with reconstructed inflow of Atlantic water to Upernavik fjord (this study) and measured surface air temperatures in Upernavik (Cappelen, 2011). a) to d) Retreat rates of Upernavik 1, Upernavik 2, Upernavik 3, and Upernavik 4, respectively (Andresen et al., 2014). e) Percentage calcareous foraminifera in core POR13-05, used as a proxy for Atlantic water inflow. f) Observed surface air temperatures in
5 Upernavik (Cappelen, 2011).